Resonance heat transfer during the forced convection of the Al_2O_3 nanofluid in a horizontal channel with a heat sink

Abdelouahab Bouttout

National Center of Building Integrated Studies and Research (CNERIB), Algiers, People's Democratic Republic of Algeria,
e-mail: bouttout@gmail.com,
ORCID iD: https://orcid.org/0000-0003-3907-0471

https://doi.org/10.5937/vojtehg72-48521

FIELD: mechanical engineering
ARTICLE TYPE: original scientific paper

Abstract:

Introduction/purpose: The continuous advancements in electronic device technologies have led to increased power densities, resulting in substantial heat generation during their operation. Efficient thermal management is essential to maintain optimal performance, prolong device lifespan, and prevent thermal-induced failures. Traditional cooling methods, such as air and liquid cooling, have reached their limitations in meeting the escalating cooling demands. Consequently, the implementation of nanofluids as a novel cooling medium has gained significant attention in recent years.

Methods: The current study aims to determine the wide band of the frequencies for which the heat transfer is maximal during the cooling of nine electronic components mounted on a horizontal channel using the Al_2O_3 nanofluid. This phenomenon is called resonance heat transfer, and it occurs when the frequency of external forcing (pulsation or oscillation) matches the natural frequency of the convective flow of the nanofluid. The finite volume method has been used to solve the governing equation. Two cases are considered in this work: uniform and pulsed inlet flow. The electronic components have been considered as heated blocks with the same space between them.

Results: The results show that the flow is unstable for the critical Reynolds number Re≈2000 Al_2O_3 nanofluid with frequency as the Strouhal number St=1.2 and a fraction concentration of 0.10. It corresponds to a flow velocity of 0.211 m/s and a dominant frequency of fr=34 Hz.

Conclusions: The enhanced heat transfer is calculated as the rate of Nusselt number of pulsation flow with the Nusselt number of uniform flow. An enhanced heat transfer rate can be achieved 30-170 % within a band of the Strouhal number St=[0.2-1.2] corresponding to a band of frequency fr =[12-34] Hz.

Key words: nanofluid, resonance, heat transfer, heat sink, convection, Strouhal number.

Introduction

In many industrial applications, heat flux is amplified due to the complexity of manufacturing processes. In such instances, various equipment and components exhibit sensitivity to variations in temperature during their operation. In order to keep the functionality of components in their temperature level, it is important to transport calories away from hot spot locations. In electronic components, the heat flux dissipation of CPU can achieve 110-140 W; it increases significantly with input voltage and frequency (Putra et al, 2011). Bar-Cohen, A. (1987) showed that durability can be improved significantly by operating a device with reasonable temperature below 85 °C. In addition, the reliability of silicon chips can decrease by 50 % for every 10 °C temperature rise. In addition to change in the architectural configuration of heat exchangers such as chaps and roughness of surfaces in order to increase heat transfer rate, it is important to modify the physical characteristics of the fluid (Bar-Cohen et al, 2007). Nanofluid particles dispersed in the base fluid demonstrate a good heat transfer transport phenomena (Choi & Eastman, 1995). Nanofluids are engineered suspensions of nanometer-sized solid particles or nanoparticles in a base fluid, exhibiting extraordinary thermophysical properties compared to conventional cooling fluids. The combination of nanoparticles and base fluids results in an enhanced heat transfer coefficient and improved thermal conductivity, making nanofluids promising candidates for efficient cooling. Abchouyeh et al. (2019) studied the heat transfer and nanofluid flow around four sinusoidal side obstacles in a horizontal channel using the Lattice Boltzman Method LBM. The effects of the Reynolds number and the nanoparticles volume fraction at different nondimensional amplitudes of the wavy wall of sinusoidal obstacles are studied. An increase of the Reynolds number leads to a rise of the temperature gradient on the channel walls. An increment of nanoparticles concentration results in the heat transfer enhancement. Mohammed et al. (2015) present the laminar mixed convection flow of Al_2O_3/water nanofluids through two hot obstacles mounted on the bottom wall of a horizontal channel. The effect on heat transfer of different parameters such as the Richardson number, the Rayleigh number, the nanoparticles volume fraction and the aspect ratios of obstacles are examined. Their results show that the difference between the average Nusselt numbers obtained from the three sets of thermophysical models does not exceed 3%. In addition, the increase of the nanofluid concentration from 0% to 5% leads to an increase lower than 10% of the average Nusselt number over the obstacles.

Mohammed et al. (2015) present a summary of experimental and numerical works of heat transfer enhancement through facing step and corrugated channels using conventional fluids and nanofluids. Laminar and turbulent flows regimes through facing step and corrugated channels are presented. Their previous works show good agreement between numerical and experimental studies to enhance heat transfer. The corrugated facing step channel is a new design proposed to enhance heat transfer rate. The heat transfer enhancement was evaluated up to 60% when using nanofluid in the facing step channel configurations. Regression equations can correlate relationships between the Nusselt number and the flow parameters. The friction factor is an important parameter to calculate the pressure drop through the inlet and the outlet of the corrugated channel and keep optimum heat transfer enhancement.

Pishkar & Ghasemi (2012) present a numerical study of laminar mixed convection in a horizontal channel using pure water and Cu-water nanofluid over two blocks mounted on the bottom wall heated at a constant temperature. Different parameters are studied: the Reynolds and the Richardson numbers, the solid volume fraction, and the distance and the thermal conductivity of the blocks. The distance and the thermal conductivity of the blocks have a significant effect on the heat transfer rate. The influence of the solid volume fraction on the increase of heat transfer is clearer at a higher Reynolds number.

Bouttout et al. (2014) studied numerically hydrodynamic amplification and thermal instabilities by imposing pulsation during forced convection of air cooling of nine identical heated blocks mounted on a horizontal channel. The new feature of this work is that a narrowband of frequencies where the enhancement of heat transfer of all electronic components is in the range of 25%-55% compared with steady non-pulsation flow is obtained. Good agreement between numerical simulations and experimental results available from literature is obtained. Recently, Bouttout, A. (2023) investigated the forced convection flow of air through a power supply box with a piezoelectric fan of nine identical electrical devices. The efficiency of the piezoelectric fan is expressed by the maximum temperature of the ninth electrical device which does not exceed 80 °C for a time-averaged velocity of 0.556 m/s and a vibration frequency of 34.75 Hz of the piezoelectric fan. The pressure drop and the power pumping of the piezoelectric fan are obtained for different Reynolds numbers. The power loss was 4.6 times higher than that of the piezoelectric fan at re=500.

The present work examines the combination of the two methods such as an active method (pulsation of the fluid at the entrance of the channel) with a passive method (the addition of Al_2O_3 nanoparticles in the base fluid). We numerically simulated the existence of a large band of frequencies for which the heat transfer is maximal and proved the existence of resonance heat transfer using nanofluid. The resonance heat transfer occurs when the frequency of external forcing (pulsation or oscillation) matches the natural frequency of the nanofluid or the system. When this resonance condition is met, the nanofluid experiences significant energy transfer, leading to enhanced heat dissipation capabilities. It is crucial to note that employing acoustic waves with higher frequencies in an axial flow can promote the occurrence of resonant heat transfer within electronic systems.

Electronic cooling system and a physical model

The miniaturization in electronic chips has contributed to heavy pressure on the heat transfer process, in which huge heat must be effectively removed to protect the components from dangerous peak temperatures, and kept lower than 85 °C (Bar-Cohen, 1987).

The electronic components can be considered as small chips or protruding blocks which dissipate the heat during electrical current circulation.

In most practical situations, electronic components are mounted on a horizontal channel or embedded inside packaging and enclosures. Electronic components are made with ceramic, silver, nickel and copper; generally, components are mounted on a Printed Circuit Board, PCB, with copper materials (Young & Vafai, 1998). The solders fusible metal alloys are used to attach electronic components to the printed circuit board. During any peak of current, this junction has the potential to deteriorate, and protective measures should be implemented to safeguard the component. The most commonly used solders are tin-silver-copper (SAC) alloys.

The general outline of the steps and configurations involved in the transition from a real electronic cooling heat sink model to physical models integrated into a Fortran program using the finite volume method is:

- Real Electronic Cooling Heat Sink Model: The process begins with the real electronic cooling heat sink which is a physical prototype or system used for cooling electronic components to dissipate heat.

This model is based on the actual geometry and material properties of the heat sink (Figure 1 (a), (b)). The various configurations of microchannels MCHSs with heat sink and pin fins are accurately represented as real models, as depicted in Figure 2(a) and Figure 2(b).

- Geometric Representation: The geometry of the real heat sink is represented using appropriate mathematical models. This representation may include 2D or 3D geometric elements, such as polygons or meshes, depending on the complexity of the heat sink (Figure 3).
- Material Properties: The material properties of the heat sink, such as thermal conductivity and specific heat capacity, are considered to model the heat transfer within the system.
- Finite Volume Method (FVM): The finite volume method is chosen as the numerical technique for solving the heat transfer equations within the heat sink. The FVM divides the domain into control volumes and discretizes the governing equations to solve for temperature distribution and heat transfer rates.
- Numerical Solver: A Fortran program is developed to implement the finite volume method and solve the discretized heat transfer equations iteratively. The solver calculates temperature profiles and heat transfer rates for heat sink.
- Model Validation: The results obtained from the Fortran program are compared with experimental data or analytical solutions from simplified cases to validate the accuracy of the model.
- Optimization: The physical models may be further optimized based on the simulation results to improve the heat sink's design and performance (maximum temperature of heat sink, power pumping of the nanofluid and pressure loss).

By integrating the real electronic cooling heat sink model into a Fortran program using the finite volume method, engineers can efficiently analyze and optimize the thermal behavior of electronic components to design more effective cooling solutions.

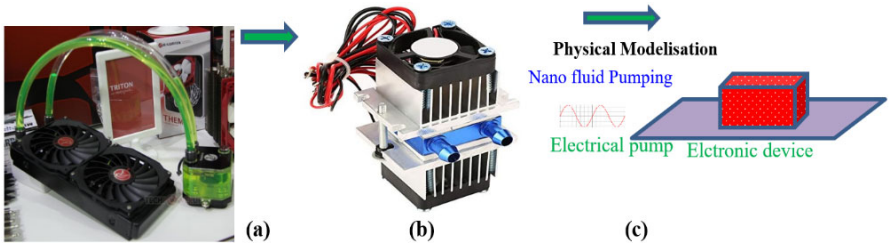

Figure 1 – Water cooling kit (a), DIY semiconductor water cooling systems (b), and modeling of electronic devices with a nanofluid pumping flow (c). The water-cooling system is used when the heat generated by the CPU is high, and classical cooling techniques with air are not sufficient.

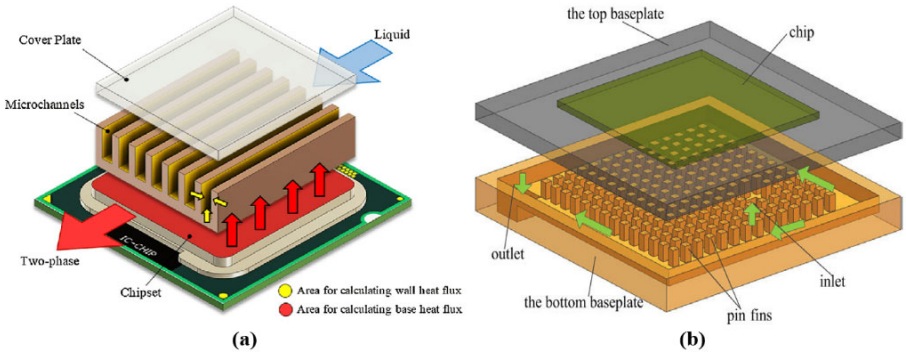

Figure 2 – Various configurations of microchannel heat sinks, MCHSs (a) straightforward channel, (b) pin fins. MCHSs combine the advantageous features of efficient electronic device operation, increased surface area per unit volume, enhanced heat transfer, and economically viable fabrication processes.

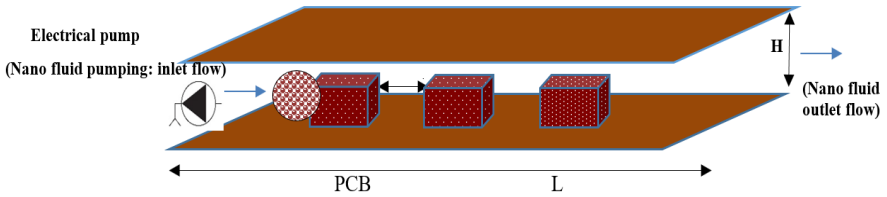

Figure 3 – General sketch of the physical model: electrical pump, electrical devices mounted on the printed circuit board (PCB) packaging. The Al_2O_3 nanofluid is used as coolant fluid. Heat in the electrical components is produced through the Joule effect occurring when electrical current passes through them. H=0.0074 m.

Mathematical formulation

The heat sink system is considered as heat convection in channels and enclosures with different configurations of heated blocks. The effects of the important parameters such as the Reynolds numbers, the Grashof number, thermal conductivity, the aspect ratio of the channel, the pitch ratio of the blocks and the method of heating on heat transfer have been examined in many works.

The following characteristics for the cooling process using nanofluids are considered:

1. No agglomeration during flow: The assumption of no agglomeration of nanoparticles ensures that they remain uniformly dispersed in the base fluid throughout the cooling system. This uniform distribution is crucial for achieving consistent and enhanced heat transfer performance.
2. The same temperature of the fluid and the particles: By assuming that the nanofluid reaches thermal equilibrium, we can consider the fluid and nanoparticles to have the same temperature. This assumption simplifies the analysis and allows us to treat the nanofluid as a single-phase medium with enhanced thermophysical properties.
3. Neglecting viscous dissipation: Viscous dissipation refers to the conversion of mechanical energy into heat due to fluid friction. Neglecting this effect implies that the energy losses due to viscous effects are insignificant, simplifying the heat transfer analysis further.

The flow through the channel is assumed to be two-dimensional, unsteady and laminar. The dimensionless variables are defined:

$$X=\frac{x}{H},\quad Y=\frac{y}{H}\ ,\ U=\frac{u}{u_0},\quad V=\frac{v}{u_0}$$
$$\tau=\frac{t.u_0}{H},P=\frac{p-p_0}{\rho_0 u_0^{\ 2}},\quad \theta=\frac{T-T_0}{Ts-T_0}\ ,\ v^*=\frac{\nu}{\nu_a} \tag{1}$$

The Nusselt number of each heated block (electronic component) is expressed in terms of the given heat flux, the measured surface temperature and the inlet temperature. It is defined as follows:

$$Nu = \frac{h.H}{k} \tag{2}$$

$$Nu = \frac{q.(H/k)}{(T_S - T_a)} \tag{3}$$

where *u* and *v* are the velocity components in the x and y directions, respectively. H is the height of the channel and t is the time.

With neglect of viscous dissipation and buoyancy force, the governing differential equations in the dimensionless form can be expressed as:

$$\frac{\partial U}{\partial X} + \frac{\partial V}{\partial Y} = 0 \tag{4}$$

$$\frac{\partial U}{\partial \tau} + \frac{\partial}{\partial X}(UU) + \frac{\partial}{\partial Y}(UV) = -\frac{\partial P}{\partial X} + \frac{1}{(1-\phi+\phi\frac{\rho_s}{\rho_f})(1-\phi)^{2.5}\,\mathrm{Re}}\left\{\frac{\partial^2 U}{\partial X^2} + \frac{\partial U^2}{\partial Y^2}\right\} \tag{5}$$

$$\frac{\partial V}{\partial \tau} + \frac{\partial}{\partial X}(UV) + \frac{\partial}{\partial Y}(VV) = -\frac{\partial P}{\partial Y} + \frac{1}{(1-\phi+\phi\frac{\rho_s}{\rho_f})(1-\phi)^{2.5}\,\mathrm{Re}}\left\{\frac{\partial^2 V}{\partial X^2} + \frac{\partial V^2}{\partial Y^2}\right\} \tag{6}$$

$$\frac{\partial \theta}{\partial \tau} + \frac{\partial}{\partial X}(U\theta) + \frac{\partial}{\partial Y}(V\theta) = \frac{1}{(1-\phi+\phi\frac{\rho Cp_s}{\rho Cp_f})} \times \frac{2-2\phi+(1+\phi)(\frac{ks}{kf})}{2+\phi+(1-\phi)(\frac{ks}{kf})} \frac{1}{\mathrm{Re}.\mathrm{Pr}}\left\{\frac{\partial^2 \theta}{\partial X^2} + \frac{\partial^2 \theta}{\partial Y^2}\right\} \tag{7}$$

where $Re=U_0H/\upsilon= \rho U_0H/\mu$, $Pr=\nu/\alpha$ are the Reynolds and Prandl numbers, respectively.

In the computational treatment of momentum equations (3) and (4), ν^* for the block can be set to an infinitely large value such as 10^{20} to simulate solid blocks.

The density, the heat capacity and the thermal expansion coefficient of the nanofluid are defined as follows:

$$\rho_{nf} = (1-\phi)\rho_f + \phi\rho_s \tag{8}$$

$$(\rho Cp)_{nf} = (1-\phi)(\rho Cp)_f + \phi(\rho Cp)_s \tag{9}$$

$$(\rho\beta)_{nf} = (1-\phi)(\rho\beta)_f + \phi(\rho\beta)_s \tag{10}$$

The thermal conductivity of the nanofluid is defined using (Maxwell, 2010):

$$\frac{k_{nf}}{k_f} = \frac{(k_s + 2k_f) - 2\phi(k_f - k_s)}{(k_s + 2k_f) + \phi(k_f - k_s)} \tag{11}$$

The mathematical relation between the dynamic viscosity μ_{nf} of the conventional base fluid and solid nano-size particles is given by Brinkman, (1952):

$$\mu nf = \frac{1}{(1-\phi)^{2.5}}\,\mu f \tag{12}$$

μf is the dynamic viscosity of the base fluid (water).
ϕ is the volume fraction.

The initial conditions of the flow are:

$$U=V=\theta=0 \tag{13}$$

The boundary conditions are:

$$X = 0, \quad 0 \le Y \le 1, \quad U = 1 + A\,sin(2\pi St\tau), V = 0, \quad \theta = 0 \tag{14}$$

$$X = L, \quad 0 \le Y \le 1, \quad \frac{\partial U}{\partial X} = \frac{\partial V}{\partial X} = \frac{\partial \theta}{\partial X} = 0 \tag{15}$$

$$Y = 0, \quad 0 \le X \le 40, \quad \frac{\partial \theta}{\partial Y} = 0 \tag{16}$$

$$Y = 1, \quad 0 \le X \le 40, \quad \frac{\partial \theta}{\partial Y} = 0 \tag{17}$$

St: the Strouhal number (Flow pulsation frequency: dimensionless frequency) is related to frequency, the height of the heat sink system (H with m) and inlet velocity U_0 (with m/s) and pulsation frequency *f* (with Hz). The Strouhal number is used by many researchers in the literature (Moon et al, 2005, 2002; Greiner, 1991) especially to control the flow pulsation, as given by the following equation:

$$St = \frac{f.H}{\boldsymbol{U0}} \tag{18}$$

Numerical approach

The governing equations are discretized using the finite volume method while the coupling between velocity and pressure fields is done

using the SIMPLER algorithm (Patankar, 1980). The components of velocity (U and V) were stored at the staggered locations, and the scalar quantities (P and θ) were stored in the centers of these volumes.

The diffusion and the convective terms in equations (5), (6) and (7) are discretized by a second order central difference scheme. Finally, the discretized algebraic equations are solved by the line-by-line tri-diagonal matrix algorithm (TDMA).

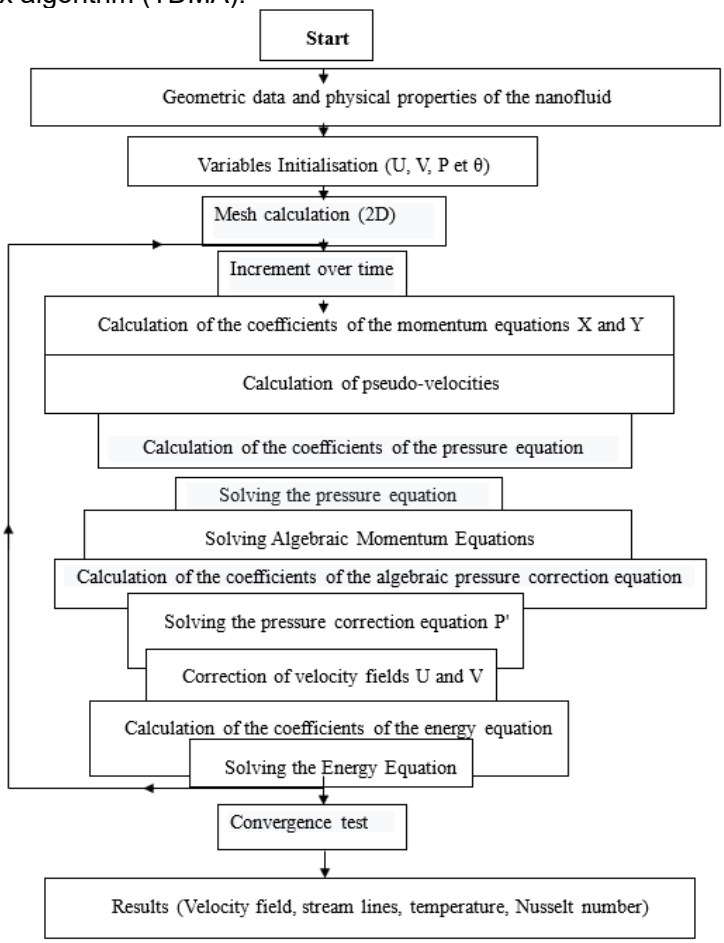

Figure 4 – Flowchart of the numerical solution using the SIMPLER Algorithm (Patankar, 1980). This flowchart presents the main steeps used to solve the coupled governing equations of the problem and to obtain the velocity field, the stream lines, the isotherms and the Nusselt number of the blocks. A Fortran program employing the finite volume method has been utilized.

A fully implicit time marching method was realized with a fixed dimensionless time step ($\Delta\tau=10^{-3}$). Convergence at a given time step is declared when the maximum change between two consecutive iteration levels falls below 10^{-4}, for U, V and θ. At this stage, the steady state solution or oscillatory regime is obtained.

This work introduces the unsteady forced convection model of nanofluid through the horizontal channel in the FORTRAN program (Afrid & Zebib,1990).

It is important to highlight that the results obtained at a specific Reynolds number were utilized as the initial conditions for computing the solutions at subsequent Reynolds numbers. For instance, the solutions obtained for Re=100 were considered as the starting point to calculate the solution for Re=200.

The Simpson rule has been used to calculate the averaged Nusselt numbers of the heated blocks by the integration over the front, top and rear surfaces of the blocks.

Figure 4 illustrates the flowchart depicting the numerical solution process utilizing the SIMPLER algorithm (Patankar, 1980).

Results and discussions

Code validation

Figure 5 shows the quantitative and qualitative validation of the code with the previous experimental and numerical works available in the literature – the experimental work of Farhanieh et al. (1993), the numerical work of Furukawa & Yang (2003) and the experimental work of Moon et al. (2005).

The different dimensional values of the configuration C2 (horizontal channel containing heated blocks) are listed in the Table 1. It is noted that (Moon et al, 2005) studied experimentally several configurations with similar dimensions of (Greiner, 1991).

The code is executed, in order to define the values of the Nusselt number of each block for different configurations and different Reynolds numbers.

It is noted that the values obtained by our numerical simulations are in good agreement compared to the results of the authors, with some differences between the geometries examined and the Reynolds number interval (cooling rate).

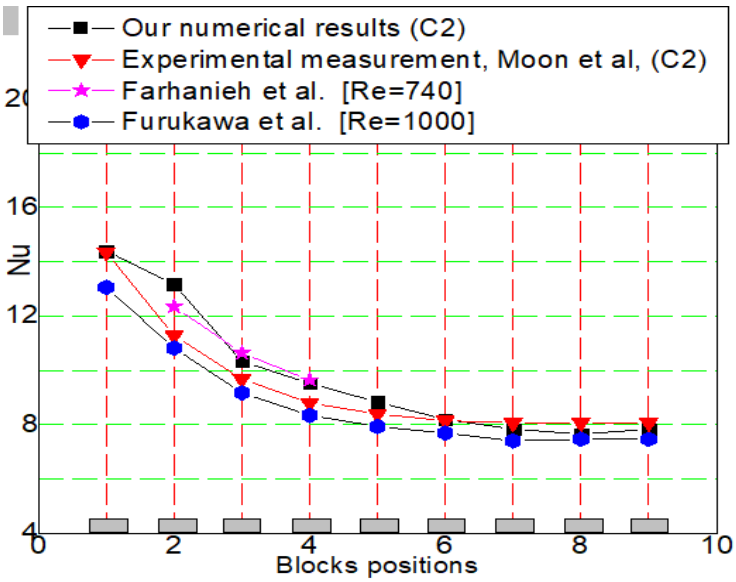

Figure 5 – Distribution of the Nusselt number along the blocks. Qualitative and quantitative comparison of our results with the previous works. The Simpson's rule has been employed to determine the average Nusselt numbers for the heated blocks by integrating across the front, top, and rear surfaces of the blocks.

Table 1 – Geometric details of the configuration. It refers to the dimensions of the geometrical block in the channel of the heat sink system

Configuration	l/L	L/H	D/h	h/H
C2	0.50	2.00	2.00	0.5

Grid and time step sensitivities

In numerical computations, conducting a grid independence study is crucial. In this study, the grid independence is examined by employing three different grid sizes for the same computational domain (502×11, 602×22, and 702×32) for Re=500 (Figure 6).

Figure 7 shows the averaged Nusselt number of the block. The number of nodes was chosen to be 602×22 after a grid-dependency test was carried out. The time step, $\Delta\tau$, was varied from 5×10^{-4} to 4×10^{-3} ($\Delta\tau$ $=2.5\times10^{-4}$, $\Delta\tau=5\times10^{-4}$, $\Delta\tau=1\times10^{-3}$, $\Delta\tau=2\times10^{-3}$ and $\Delta\tau$ $=4\times10^{-3}$); for Re=500 using a grid size of 602×22. There is the variation of the averaged Nusselt

number Nu1 of the first block with time for five various accuracies for computations.

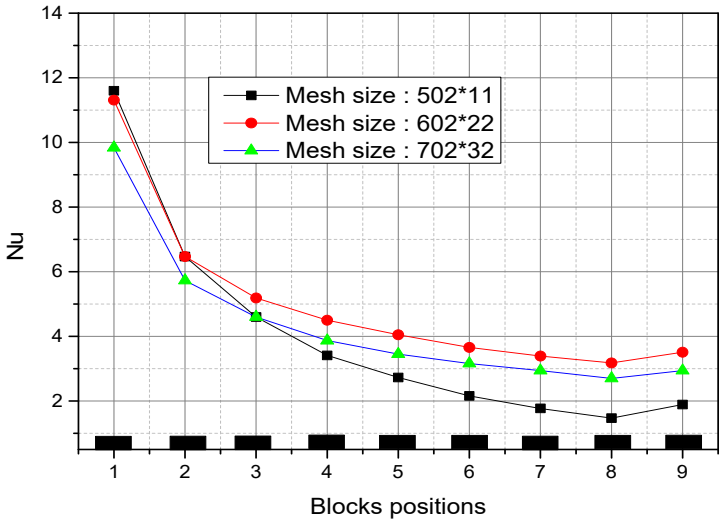

Figure 6 – Grid sensitivity for Re= 100. Φ=0.10. Grid sensitivity refers to the dependence of the solution on the size and distribution of the computational grid or mesh.

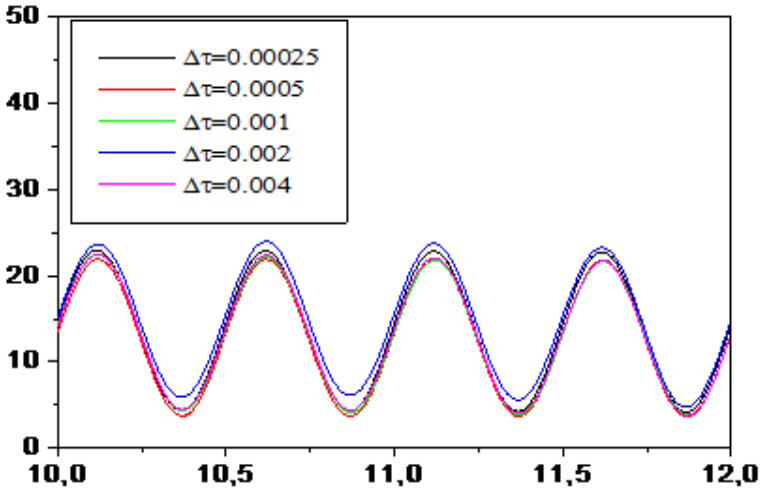

Figure 7 – Time step sensitivity for Re= 100. Φ=0.10. Convergence at a specific time step is confirmed when the maximum change between two consecutive iteration levels drops below 10^{-4} for the variables U, V, and θ. At this stage, the steady state solution or oscillatory regime is obtained.

Discussions

Steady state flow

Brownian motion exerts a significant influence on the rheological properties of nanoparticles and the thermal behavior of nanofluids. Brownian motion refers to the unpredictable stochastic movement of suspended nanoparticles, sustained by thermal diffusion; it notably intensifies at higher temperatures, smaller nanoparticle sizes, and lower viscosity. The random collision of nanoparticles in Brownian fluid environments is a fundamental factor contributing to the increased thermal conductivity of nanofluids. Additionally, a high surface-to-volume ratio of the channel with heat sinks due to reduced length scales plays a crucial role. Consequently, this phenomenon is largely confined to the interaction zone between the fluid and the surface of the channel and the heat sink, making it highly relevant.

In a steady-state flow, the fluid moves steadily and continuously without any change in velocity over time (Figure 8).

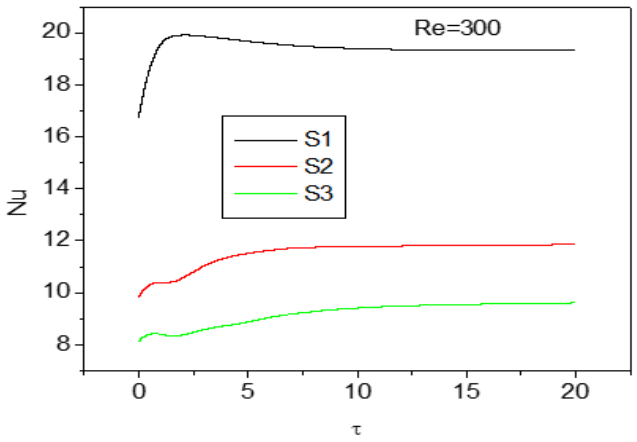

Figure 8 – Time evolution of the Nusselt number of S1, S2 and S3 for Re=300 and Φ=0.10. Steady state over time for the Nusselt number is obtained. S1, S2, and S3 denote the heat source numbers.

Stream lines flow and isotherms in the heat sink system

The streamlines and isotherms inside the system are depicted in Figure 9 for Re=500, revealing the emergence of vortices in the interlock regions of the channel. The streamlines exhibit distinct motion patterns, indicating that the flow in this area is separated from the main flow.

Notably, vortex formation is observed, suggesting specialized fluid dynamics in these regions. Additionally, the isotherm lines cluster near the blocks, and the temperature modulation induced by the voltage input frequency can disturb the thermal layer in close proximity to the blocks.

Previous studies indicate that, with an increase in the Reynolds number, the streamlines reveal a corresponding augmentation in both the size and strength of the vortices formed behind the blocks. At elevated Reynolds numbers, a robust vortex emerges, amplifying heat transfer from the surfaces of the blocks. Nevertheless, when employing the Al_2O_3 nanofluid, a distinct observation is a larger vortex formed behind the blocks. This occurrence can be attributed to the higher density and dynamic viscosity of the nanofluid. The heightened shear stress between the layers of the nanofluid contributes to the creation of a larger vortex. The velocity difference between the nanofluid and pure water is insignificant at low Reynolds numbers. However, as the Reynolds number increases, this disparity becomes more pronounced, as demonstrated in prior research (Pishkar & Ghasemi, 2012).

At low Reynolds numbers, heat transfer is primarily governed by conduction, resulting in the isotherms extending above the blocks and occupying a substantial area within the channel. As the Reynolds number increases, convection becomes the predominant heat transfer mechanism. The intensified cold inlet flow at higher Reynolds numbers pushes the isotherms closer to the bottom wall. The isotherms of the nanofluid indicate that at every point in the channel, the temperature of the nanofluid is higher. This phenomenon is attributed to the higher thermal conductivity of the nanofluid, as documented in the previous research (Pishkar & Ghasemi, 2012).

Pressures losses and power pumping

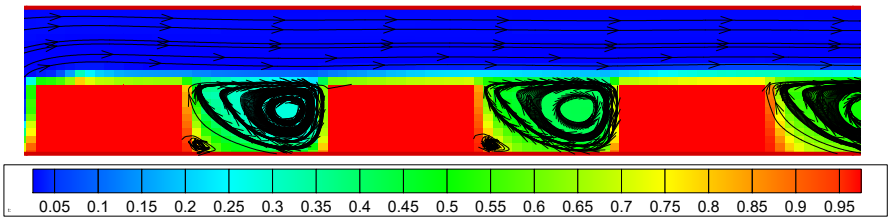

Figure 9 – Streamlines and isotherms in the section between 1st, 2nd and 3rd block. Re=500, volume fraction of Al_2O_3 nanoparticles, Φ=0.15. The streamlines exhibit distinct motion patterns, indicating that the flow in this area is separated from the main flow. The isotherm lines cluster near the blocks.

When nanofluids flow through a channel with blockages (obstacles or structures that disrupt the flow), they experience pressure losses due to fluid friction and changes in flow direction. Nanofluids typically have different rheological properties compared to conventional fluids, such as higher viscosity or different thermal conductivity. These properties affect the pressure drop across the channel. The presence of nanoparticles can alter the momentum transfer and energy dissipation in the flow, resulting in different pressure loss characteristics compared to pure base fluids.

The concentration of nanoparticles in the nanofluid plays a significant role in determining pressure loss. Higher nanoparticle concentrations can lead to increased viscosity and enhanced resistance to flow, resulting in higher pressure losses. On the other hand, lower nanoparticle concentrations may have minimal impact on pressure drop compared to the base fluid.

The geometry of blockages in the channel can influence pressure losses. Different blockage shapes, sizes, and arrangements will create varying flow patterns and turbulence, impacting pressure drop in the nanofluid.

Pumping power is the amount of energy required to overcome pressure losses and maintain fluid flow through the channel. In the case of nanofluids in a channel with blockages, pumping power will be influenced by the nanofluid viscosity and thermal conductivity, as well as the blockage geometry and the flow rate. Higher viscosity nanofluids may demand more pumping power compared to low viscosity fluids. Additionally, higher thermal conductivity nanofluids may help dissipate heat generated due to pressure losses, affecting the overall pumping power.

Heat transfer

The heat transfer gradually decreases and eventually reaches an asymptotic limit, indicating that the flow regime periodically develops along the solid blocks and then stabilizes into a steady state starting from the fifth block. Notably, the reduction rate of the average Nusselt number between the first and ninth blocks is approximately 50% for air cooling and 38% for nanofluid cooling (using Al_2O_3-water with a particle volume fraction Φ of 8%). Moreover, the analysis reveals that both cooling methods exhibit an overall heat transfer gain, with approximately 44% improvement observed for the upstream blocks and around 20% for the downstream blocks when using nanofluid cooling compared to air cooling. In practical scenarios, where heat-generating components are involved, the nanofluid cooling system activates and efficiently ensures temperature reduction,

indicating its potential for effective thermal management in such applications (Figure 10 and Figure 11).

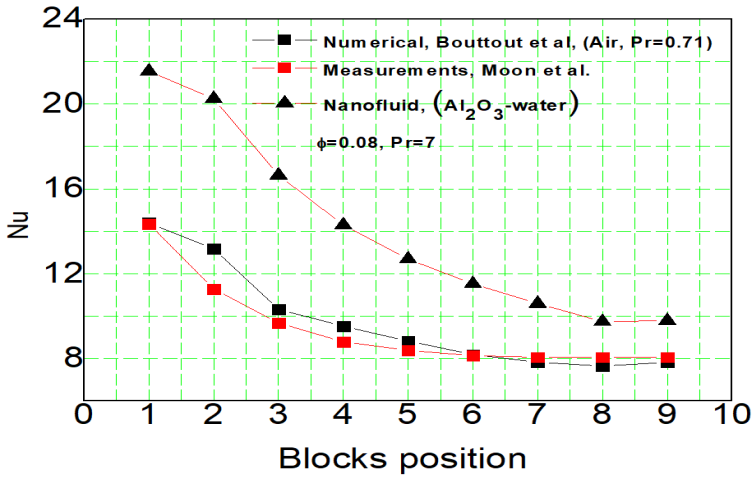

Figure 10 – Distribution of the Nusselt number along the blocks. A=0.0, Re=700 (air cooling, Pr=0.71) and cooling using a nanofluid (Al_2O_3/water - Pr=7.0, Φ=8%). Heat transfer is higher for the nanofluid in the heated sink compared to both water and air cooling methods.

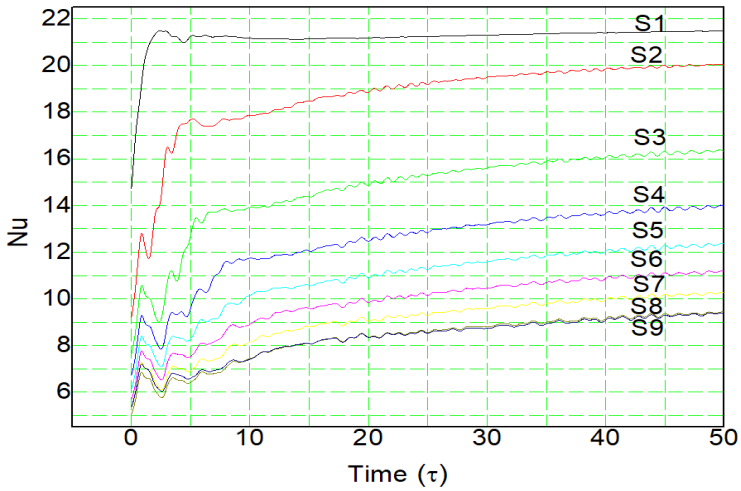

Figure 11 – Distribution of the Nusselt number along the blocks, for Re=300 and Φ=0.10. Configuration C2. The heat transfer from the heat sinks gradually decreases and eventually reaches an asymptotic limit. S1, S2, S3, S4, S5, S6, S7, S8 and S9 denote the heat source numbers.

Pulsation state flow

The numerical simulation involves employing an electrical pumping model to simulate pulsating nanofluid flow at the channel inlet. The heat sink is regarded as a heated block that receives the coolant flow to achieve functional safety temperature.

As the velocity of the nanofluid increases, the Brownian motion of the particles also intensifies, leading to a consequent enhancement in the nanofluid thermal transport capabilities. Consequently, at higher Reynolds numbers, there is a decrease in thermal resistance. Figure 12 illustrates the resonance heat transfer of the heat sink, showcasing the maximum heat transfer occurring at various positions of the heat sinks.

The maximum heat transfer factor E is determined by comparing the Nusselt number in both steady-state and unsteady pulsating conditions during the Al_2O_3 nanofluid cooling process (Figure 12). The maximum heat transfer factor, E, is expressed by the following equation:

$$E = \frac{max(Nu(St))}{\max(Nu(St{=}0))} \tag{19}$$

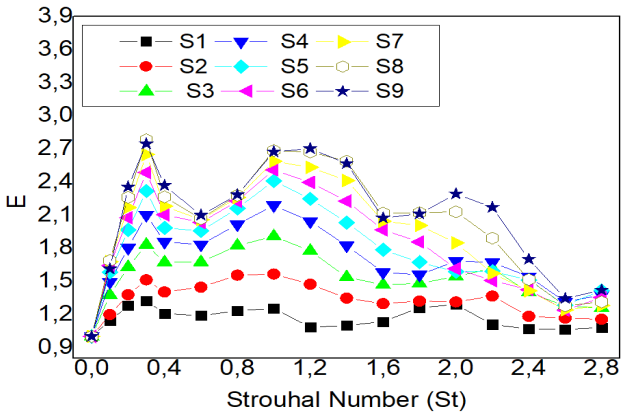

Figure 12 – Distribution of the enhancement factor of the Nusselt number E along the blocks for Re=500 and Φ=0.10. Configuration C2. It is observed that the enhancement factor of the heat sinks achieves the maximum values within a certain frequency range. This phenomenon is referred to as resonance heat transfer enhancement. S1, S2, S3, S4, S5, S6, S7, S8 and S9 denote the heat source numbers.

The results reveal the flow instability at the critical Reynolds number (Re ≈ 2000) in the Al_2O_3 nanofluid, with frequencies corresponding to the Strouhal number (St) of 1.2 and a fractional concentration of 0.10. This observation is associated with a flow velocity of 0.211 m/s and a dominant

frequency of fr = 34 Hz. Figure 13 illustrates the temporal evolution of the dimensionless vertical velocity of the nanofluid inside the heat sink system. This figure shows that the flow exhibits instability at Re ≈ 2000. In this regime, the flow transitions from a stable to an unstable regime due to the concentration of nanoparticles, heat generation by electronic components, and disrupted boundary layer through the channel. These findings provide valuable insights into the thermodynamic behavior of the system under consideration, considering variations in different parameters such as the nanoparticle concentration, the Reynolds number and the geometric configuration of different blocks within the system.

Figure 14 illustrates the Fast Fourier Transform (FFT) analysis of the vertical velocity within a heat sink system. The FFT analysis is a powerful tool for analyzing the frequency components of a signal, in this case, the temporal vertical velocity of nanofluid. It helps to identify dominant frequencies and understand the dynamics of the nanofluid flow within the heat sink. The peaks in the FFT plot indicate a dominant frequency of 34 Hz (St=1.2) at which the vertical velocity oscillates, revealing periodic oscillations due to flow instabilities. The same analysis using the FFT is employed by other authors (Afrid & Zebib,1990).

Figure 15 illustrates the temporal variation of the Nusselt number of the heat sinks blocks for Re=500 and Φ=0.10. As time increases, the influence of the velocity pulsation component of the nanofluid on the heat transfer rate for each heat sink gradually becomes more pronounced. Ultimately, the variation of the heat transfer approaches a periodic state with time $\tau \geq 10$.

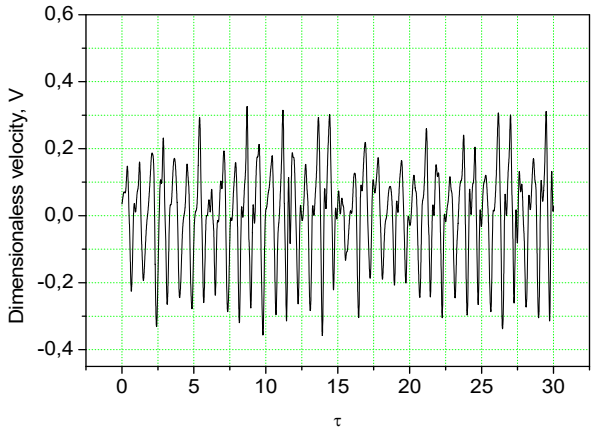

Figure 13 – Temporal evolution of the dimensionless vertical velocity of the nanofluid inside the heat sink system. Re= 2000, ϕ=0.10.

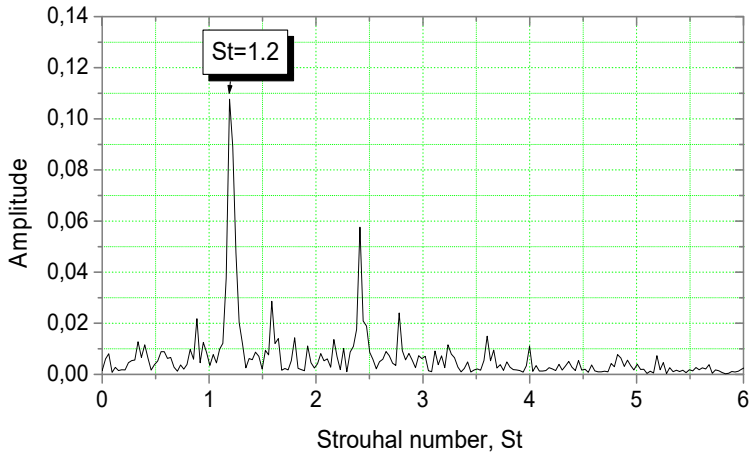

*Figure 14 – Fast Fourier Transform of the dimensionless vertical velocity of the nanofluid inside the heat sink system. Re= 2000, ϕ=0.10. St=1.2, H=0.0074m, U0=0.211 m/s, (**f**=34 Hz).*

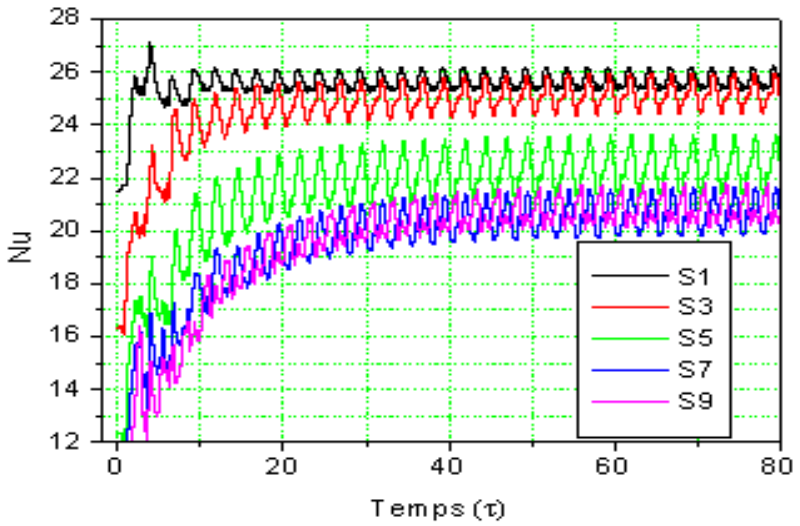

Figure 15 – Distribution of the Nusselt number along the blocks. St=1.2. Re=500 and Φ=0.10. The oscillatory convection inside the channel has been obtained. S1, S3, S5, S7 and S9 denote the heat source numbers.

Calculation of the dimensional temperatures of the heated blocks

The miniaturization in electronic chips has contributed to heavy pressure on heat transfer process, in which huge heat must be effectively removed to protect the components from the dangerous peak temperatures, and kept lower than 85 °C (Bar-Cohen, 1987).

In addition, the reliability of silicon chips can decrease by 50 % for every 10 °C temperature rise.

In the present configuration, the temperature of each electronic component has been calculated by the following formula:

$$T_S = \frac{q.(h/k)}{Nu} + T_a \quad (20)$$

where
T_s is the temperature of the heated block in °C,
q is the heat flux in W/ m^2,
h is the height of the heated block in m,
Nu is the averaged Nusselt number,
T_a is air temperature in °C (25 °C), and
k is the thermal conductivity of air W/ m.K.

In numerical simulation, we considered that conduction losses across the plate and radiation are neglected. In the practice of cooling electronic components, it is more convenient to estimate the percent dissipation of each mode to properly quantify the average Nusselt number. We consider that the heat flux per area is in the range of 110 and 140 W. The heat dissipation resulting from a processor increases significantly with the voltage and the frequency (Pishkar & Ghasemi, 2012).

It is worth noting that the majority of measurements in the literature are conducted on solid blocks heated by the Joule effect and exposed to high temperatures as in the case of aluminum blocks in the studies by (Moon et al, 2005). However, diodes and transistors mounted on electronic circuit boards typically withstand temperatures ranging from 80 to 90°C. These values depend on the nature of the electronic components and their constituent materials.

Figure 16 illustrates the temperature by varying the Reynolds number at fixed volume fractions of Al_2O_3/water nanoparticles (0.10). It has been observed that for both Al_2O_3/water nanofluids and distilled water, the Nusselt number increases with higher Reynolds numbers, indicating that the temperature of the heat block is sensitive to the Reynolds number.

Figure 17 illustrates that the temperature of the blocks of Al_2O_3/water nanofluids at the volume concentrations of 0.05, 0.10, and 0.15 experiences a significant decrease temperature of 66 °C, 61°C, and 56°C, respectively for the 8th block. This decrease in the temperature is attributed to the greater participation of nanoparticles in the nanofluids, leading to a notable enhancement of thermal conductivity. In essence, the higher the concentration of nanoparticles in nanofluids, the greater the improvement in thermal conductivity, resulting in elevated Nusselt numbers.

The study conducted by (Putra et al, 2011) concluded that the most favorable outcomes were achieved when employing Al_2O_3-water nanofluids. Under an inlet temperature of 30 °C, the average CPU temperature, utilizing water as a coolant in the heat pipe liquid block, was recorded at 39.7 °C. In contrast, temperatures for Al_2O_3-water were measured at 38.5 °C and 37.8 °C for the volume fractions of 0.5% and 1.0%, respectively (Putra et al, 2011).

The pulsation of nanofluids within electronic systems leads to a substantial improvement in heat and mass transfer. This enhancement is attributed to mechanical agitation and micro-convection, particularly facilitated by the Brownian motion of alumina nanoparticles suspended in the base fluid. The pulsation promotes micro-convection along the boundary layer over the surfaces of electronic components at different frequencies, further optimizing heat and mass transfer in the system.

The increase in the volume fraction of nanoparticles (Al_2O_3) in the base fluid (water) leads to an enhancement in the Nusselt number. Additionally, the increase in nanoparticles results in an improvement in the conductive heat transfer coefficient, while the augmentation of mass motion of the fluid contributes to enhanced heat transfer. The same results are obtained by other authors using the Al_2O_3 nanofluid as a cooling fluid inside a rectangular ribbed channel (Parsaiemehr et al, 2018).

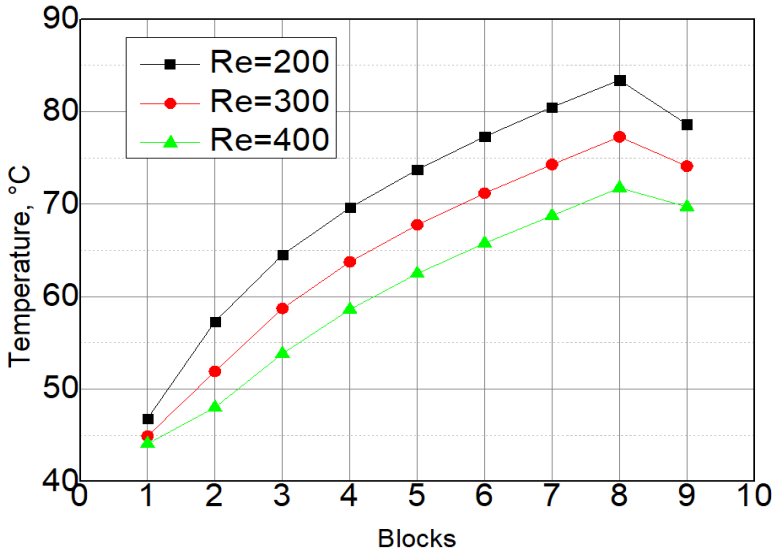

Figure 16 – Distribution of temperature along the blocks for different Reynolds numbers. ϕ=0.15. The increase in Reynolds numbers leads to a decrease in the temperature of heat sinks, resulting in better cooling performance for thermal systems.

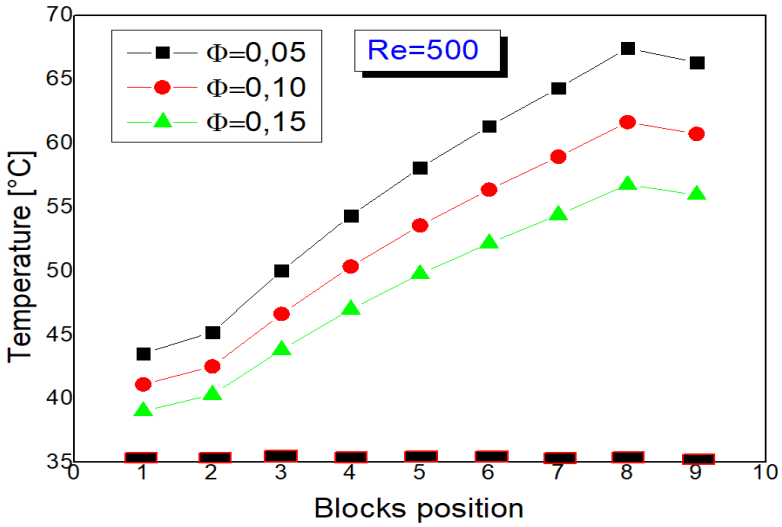

Figure 17 – Distribution of temperature along the blocks for different nanofluid concentrations. The increase in nanofluid concentration leads to a decrease in the temperature of heat sinks, resulting in better cooling performance for thermal systems.

Conclusion

The growing performance capabilities of electronic devices have led to a corresponding increase in generated heat, necessitating effective thermal management systems for maintaining optimal operating temperatures. Nanofluid cooling presents a compelling and innovative solution for tackling thermal challenges faced by modern electronic devices. Continued research and development in this area have the potential to revolutionize thermal management and significantly improve the performance and reliability of electronic systems across various industries.

The findings of the paper can be summarized as follows:

- The forced convection flow of a nanofluid with and without pulsation at the entrance of a channel equipped with electronic components has been studied numerically. The nanofluid models are introduced into the Navier-Stokes equations coupled with the energy equation.
- The results show that the pulsation of the nanofluid (10% by volume of Al_2O_3 particles), with 50% of the mean flow and with the Strouhal number range of [0.2-1.2], leads to an increase in heat transfer of approximately 30% to 170%. As a result, there is improved cooling of electronic components.
- Nanofluids, which include Al_2O_3 in water, and which are subjected to a pulsation frequency range of [12-34] Hz, exhibit significant temperature reductions at volume concentrations of 0.05, 0.10, and 0.15. On average, a notable decrease of 60 °C is observed across the blocks.
- During nanofluids flow inside an electronic system, the heat and mass transfer can be improved remarkably as a result of mechanical agitation and micro-convection created principally by the Brownian motion of alumina nanoparticles in the base fluid.
- The results of this study can be used to optimize the pumping power of the nanofluid and precisely size the cooling pumps for electronic systems, as well as to control their operating temperatures effectively.
- In the perspective of this study, it is recommended to investigate the impact of acoustic excitation on enhancing the cooling performance of a heat sink using a nanofluid. The analysis should focus on studying the frequency of acoustic excitation and its effects on nanoparticle dispersion within the nanofluid, as well as the resulting Brownian motion, contributing to enhanced heat transfer.

References

Abchouyeh, M.A., Fard, O.S., Mohebbi, R. & Sheremet, M.A. 2019. Enhancement of heat transfer of nanofluids in the presence of sinusoidal side obstacles between two parallel plates through the lattice Boltzmann method. *International Journal of Mechanical Sciences*, 156, pp.159-169. Available at: https://doi.org/10.1016/j.ijmecsci.2019.03.035.

Afrid, M. & Zebib, A. 1990. Oscillatory three-dimensional convection in rectangular cavities and enclosures. *Physics of Fluids A: Fluid Dynamics*, 2(8), pp.1318-1327. Available at: https://doi.org/10.1063/1.857582.

Bar-Cohen, A., Wang, P. & Rahim, E. 2007. Thermal management of high heat flux nanoelectronic chips. *Microgravity Science and Technology*, 19, pp.48-52. Available at: https://doi.org/10.1007/BF02915748.

Bar-Cohen, A. 1983. Thermal Frontiers in the Design and Packaging of Microelectronic. *Equipment Mechanical Engineering*, 150, art.number:53 [online]. Available at: https://cir.nii.ac.jp/crid/1570572699153144192 [Accessed: 02 January 2024].

Bouttout, A. 2023. Forced Convection during Cooling of Power Supply Box using Pulsation Flow with Piezoelectric Fan. *IEEJ Transactions on Electrical and Electronic Engineering*, 18(6), pp.865-875. Available at: https://doi.org/10.1002/tee.23800.

Bouttout, A., Benissaad, S. & Bessaïh, R. 2014. Numerical Study of Forced Convection in a Horizontal Channel with Heated Blocks Due to Oscillation of Incoming Flow. *Numerical Heat Transfer, Part A: Applications*, 65(6), pp.584-600. Available at: https://doi.org/10.1080/10407782.2013.836013.

Brinkman, H.C. 1952. The Viscosity of Concentrated Suspensions and Solutions. *The Journal of Chemical Physics*, 20(4), art.number:571. Available at: https://doi.org/10.1063/1.1700493.

Choi, S.U.S. & Eastman, J.A. 1995. Enhancing thermal conductivity of fluids with nanoparticles. In: *International mechanical engineering congress and exhibition*, San Francisco, CA, USA, November 12-17 [online]. Available at: https://www.osti.gov/biblio/196525 [Accessed: 02 January 2024].

Farhanieh, B., Herman, Č. & Sundén, B. 1993. Numerical and experimental analysis of laminar fluid flow and forced convection heat transfer in a grooved duct. *International Journal of Heat and Mass Transfer*, 36(6), pp.1609-1617. Available at: https://doi.org/10.1016/S0017-9310(05)80070-5.

Furukawa, T. & Yang, W.-J. 2003. Thermal-fluid flow in parallel boards with heat generating blocks. *International Journal of Heat and Mass Transfer*, 46(26), pp.5005-5015. Available at: https://doi.org/10.1016/S0017-9310(03)00357-0.

Greiner, M. 1991. An experimental investigation of resonant heat transfer enhancement in grooved channels. *International Journal of Heat and Mass Transfer*, 34(6), pp.1383-1391. Available at: https://doi.org/10.1016/0017-9310(91)90282-J.

Maxwell, J.C. 2010. *A Treatise on Electricity and Magnetism, Volume 1*. Cambridge University Press. Available at: https://doi.org/10.1017/CBO9780511709333.

Mohammed, H.A., Alawi, O.A. & Wahid, M.A. 2015. Mixed convective nanofluid flow in a channel having backward-facing step with a baffle. *Powder Technology*, 275, pp.329-343. Available at: https://doi.org/10.1016/j.powtec.2014.09.046.

Moon, J.W., Kim, S.Y. & Cho, H.H. 2005. Frequency-dependent heat transfer enhancement from rectangular heated block array in a pulsating channel flow. *International Journal of Heat and Mass Transfer*, 48(23-24), pp.4904-4913. Available at: https://doi.org/10.1016/j.ijheatmasstransfer.2005.06.006.

Moon, J.W., Kim, S.Y. & Cho, H.H. 2002, January. An Experimental Study on Forced Convection From a Rectangular Heated Block by Acoustic Excitation in a Channel Flow. In: *ASME International Mechanical Engineering Congress and Exposition,* New Orleans, Louisiana, USA, paper no:IMECE2002-33721, pp.81-88, November 17-22. Available at: https://doi.org/10.1115/IMECE2002-33721.

Parsaiemehr, M., Pourfattah, F., Akbari, O.A., Toghraie, D. & Sheikhzadeh, G. 2018. Turbulent flow and heat transfer of Water/Al_2O_3 nanofluid inside a rectangular ribbed channel. *Physica E: Low-Dimensional Systems and Nanostructures*, 96, pp.73-84. Available at: https://doi.org/10.1016/j.physe.2017.10.012.

Patankar, S. 1980. *Numerical Heat Transfer and Fluid Flow, 1st Edition*. Boca Raton: CRC press. Available at: doi.org/10.1201/9781482234213.

Pishkar, I. & Ghasemi, B. 2012. Cooling enhancement of two fins in a horizontal channel by nanofluid mixed convection. *International Journal of Thermal Sciences*, 59, pp.141-151. Available at: https://doi.org/10.1016/j.ijthermalsci.2012.04.015.

Putra, N., Yanuar,nd & Iskandar, F.N. 2011. Application of nanofluids to a heat pipe liquid-block and the thermoelectric cooling of electronic equipment. *Experimental Thermal and Fluid Science*, 35(7), pp.1274-1281. Available at: https://doi.org/10.1016/j.expthermflusci.2011.04.015.

Young, T.J. & Vafai, K. 1998. Convective flow and heat transfer in a channel containing multiple heated obstacles. *International Journal of Heat and Mass Transfer*, 41(21), pp.3279-3298. Available at: https://doi.org/10.1016/S0017-9310(98)00014-3.

Transferencia de calor por resonancia durante la convección forzada del nanofluido Al_2O_3 en un canal horizontal con disipador de calor

Abdelouahab Bouttout

Centro Nacional de Estudios e Investigaciones Integradas de la Construcción (CNERIB), Argel, República Argelina Democrática y Popular

CAMPO: ingeniería mecánica
TIPO DE ARTÍCULO: artículo científico original

Resumen:

Introducción/objetivo: Los continuos avances en las tecnologías de dispositivos electrónicos han llevado a mayores densidades de energía, lo que resulta en una generación sustancial de calor durante su funcionamiento. La gestión térmica eficiente es esencial para mantener un rendimiento óptimo, prolongar la vida útil del dispositivo y prevenir fallas inducidas térmicamente. Los métodos de enfriamiento tradicionales, como el enfriamiento por aire y por líquido, han alcanzado sus limitaciones a la hora de satisfacer las crecientes demandas de enfriamiento. En consecuencia, la implementación de nanofluidos como un nuevo medio de enfriamiento ha ganado mucha atención en los últimos años.

Métodos: El presente estudio tiene como objetivo determinar la banda ancha de frecuencias para las cuales la transferencia de calor es máxima durante el enfriamiento de nueve componentes electrónicos montados en un canal horizontal utilizando el nanofluido Al_2O_3. Este fenómeno se llama transferencia de calor por resonancia y ocurre cuando la frecuencia del forzamiento externo (pulsación u oscilación) coincide con la frecuencia natural del flujo convectivo del nanofluido. Se ha utilizado el método del volumen finito para resolver la ecuación gobernante. En este trabajo se consideran dos casos: flujo de entrada uniforme y pulsado. Los componentes electrónicos se han considerado como bloques calentados con el mismo espacio entre ellos.

Resultados: Los resultados muestran que el flujo es inestable para el nanofluido crítico con número de Reynolds $Re \approx 2000$ Al_2O_3 con una frecuencia como el número de Strouhal St = 1.2 y una concentración de fracción de 0.10. Corresponde a una velocidad de flujo de 0.211 m/s y una frecuencia dominante de fr=34 Hz.

Conclusión: La transferencia de calor mejorada se calcula como la relación del número de Nusselt de flujo pulsante con el número de Nusselt de flujo uniforme. Se puede lograr una tasa de transferencia de calor mejorada del 30 al 170 % dentro de una banda del número de Strouhal St = [0.2-1.2] correspondiente a una banda de frecuencia fr = [12-34] Hz.

Palabras claves: nanofluido, resonancia, transferencia de calor, disipador de calor, convección, número de Strouhal.

Резонансный теплообмен при принудительной конвекции наножидкости Al_2O_3 в горизонтальном канале с системой охлаждения

Абделуахаб Буттаут

Национальный центр комплексных исследований в области строительства (CRIB),
г. Алжир, Алжирская Народная Демократическая Республика

РУБРИКА ГРНТИ: 27.35.45 Математические модели теплопроводности и диффузии,
30.17.00 Механика жидкости и газа
ВИД СТАТЬИ: оригинальная научная статья

Резюме:

Введение/цель: Постоянный технологический прогресс электронных устройств привел к повышению плотности электрической энергии, которая, в свою очередь, выделяет значительное количество тепла во время эксплуатации. Эффективное управление температурным режимом необходимо для поддержания оптимальной производительности, продления срока службы устройства и предотвращения поломок, вызванных перегревом. Традиционные методы охлаждения с помощью воздуха и жидкости не отвечают возросшим потребностям в охлаждении. Вследствие чего применение наножидкостей в качестве нового охлаждающего средства в последнее время приобретает большую значимость.

Методы: Целью данного исследования является определение широкого диапазона частот в условиях максимального теплообмена при охлаждении девяти электронных компонентов, установленных на горизонтальном канале, с помощью наножидкости Al_2O_3. Это явление называется резонансной теплопередачей и возникает, когда частота внешнего воздействия (пульсации или колебания) совпадает с собственной частотой конвективного течения наножидкости. Для решения основного уравнения использовался метод конечных объемов. В данной статье рассматриваются два случая: равномерный и пульсирующий входной поток. Электронные компоненты представляют собой блоки, которые нагреваются и расположены на равном расстоянии друг от друга.

Результаты: Результаты исследования показали, что течение неустойчиво при критическом числе Рейнольдса Re≈2000 для наножидкости Al_2O_3 с частотой, равной числу Струхаля St = 1,2, и концентрацией фракции 0,10. Это соответствует скорости потока 0,211 м/с и преобладающей частоте fr = 34 Гц.

Вывод: Улучшенная теплопередача рассчитывается как соотношение числа Нуссельта для пульсирующего потока и числа Нуссельта для равномерного потока. Повышенная скорость теплопередачи может быть достигнута на 30-170% в диапазоне чисел Струхаля St = [0,2-1,2], соответствующем диапазону частот fr = [12-34] Гц.

Ключевые слова: наножидкость, резонанс, теплопередача, система охлаждения, конвекция, число Струхаля.

Резонантни пренос топлоте током форсиране конвекције нанофлуида Al_2O_3 у хоризонталном каналу са хладњаком

Абделуахаб Бутаут

Национални центар за изградњу интегрисаних студија и истраживања (CNERIB), Алжир, Народна Демократска Република Алжир

ОБЛАСТ: машинство
КАТЕГОРИЈА (ТИП) ЧЛАНКА: оригинални научни рад

Сажетак:

Увод/циљ: Стални напредак у технологијама електронских уређаја довео је до повећаних густина електричне енергије што производи знатне количине топлоте током њиховог рада. Ефикасно управљање топлотом је суштинско за одржавање оптималних перформанси, продужавање века трајања уређаја, као и за спречавање кварова узрокованих топлотом. Традиционалне методе хлађења, на пример ваздухом и течношћу, нису више у стању да прате повећане потребе за хлађењем. Зато примена нанофлуида, као новог расхладног средства, у последње време добија на значају.

Методе: Циљ ове студије јесте да одреди широки опсег фреквенција за које је пренос топлоте максималан током хлађења девет електронских компонената постављених на хоризонтални канал помоћу нанофлуида Al_2O_3. Ова појава се назива резонантни пренос топлоте и до ње долази када се фреквенција спољашње принуде (пулсирања или осцилације) поклапа са природном фреквенцијом конвективног тока нанофлуида. Метода коначних запремина коришћена је у решавању водеће једначине. Разматрана су два случаја: униформни и пулсни улазни проток. Електронске компоненте представљају блокове који се греју и налазе се на подједнаком растојању једни од других.

Резултати: Показано је да је проток нестабилан за критични Рејнолдсов број $Re\approx2000$ нанофлуида Al_2O_3 са фреквенцијом као Строхаловим бројем $St=1,2$ и концентрацијом фракција од 0,10, што одговара брзини протока од 0,211 m/s и доминантној фреквенцији од $fr=34$ Hz.

Закључак: Повећани пренос топлоте израчунава се као брзина Нуселтовог броја пулсног протока са Нуселтовим бројем равномерног протока. Повећана брзина преноса топлоте може се постићи 30–70% унутар опсега Строхаловог броја $St=[0,2–1,2]$, што одговара опсегу фреквенције $fr=[12–34]$ Hz.

Кључне речи: нанофлуид, резонанција, пренос топлоте, хладњак, конвекција, Строхалов број.

Paper received on: 02.01.2024.
Manuscript corrections submitted on: 16.11.2024.
Paper accepted for publishing on: 18.11.2024.